A critical assessment of the convergent-beam electron diffraction technique used for determining elastic strain in semiconductor superlattices

Mogili, N.V.V.[1], Tanner, D.A.[2] and Nakahara, S.[2]

[1] Brazilian Nanotechnology National Laboratory, Centro Nacional de Pesquisa em Energia e Materiais, Brazil, [2] Bernal Institute, University of Limerick, Ireland

An ability to determine the elastic strain state of semiconductor devices could not only offer an important diagnostic step for semiconductor processing, but also open an opportunity in developing new advanced devices. At present, a scanning transmission electron microscope (STEM) equipped with a field emission gun is probably the available tool that is capable of performing such a strain analysis with high spatial resolution. In the STEM, a convergent-beam electron diffraction (CBED) method in combination with computer simulation can be used to make a nano-scale local strain analysis, in which the magnitude of an elastic strain is evaluated using the shift of HOLZ (higher-order Laue zone) diffraction lines. Here an attempt is made to assess the accuracy of the CBED method using a controlled <001> silicon sample containing five layers of germanium-silicon/silicon (Ge-Si/Si) strained superlattice (SSL). It will be shown that the spatial resolution of strain measurements by CBED is affected primarily by the beam size [1].

Figure 1 is a bright-field STEM image showing the (110) cross section of the Si sample containing five layers of Ge-Si/Si superlattice. A convergent beam spot over the cross section produces a HOLZ pattern characteristic of a zone of interest. These patterns obtained at 10 to 12 spots across the #1 Ge-Si layer are compared with computer simulation, and finally the magnitude of the principal strain, $\bar{\varepsilon}_{xx}$, is determined along the x direction, i.e. [001] (see Fig. 1). The bar sign over the strain means that the strain is averaged over the specimen thickness. Finally, an elasticity solution for the present SSL configuration was formulated using a Fourier-series method [2]. In Fig. 2, the experimental strains, $\bar{\varepsilon}_{xx}$, are plotted and compared with the theoretical plot, and a significant difference can be observed between them. The experimental strain curve consists of a flat-top (FT) region surrounded by two symmetrical shoulders with a gradually-declining slope, whereas the corresponding theoretical strain profile is almost a square step with nearly vertical shoulders. From the shape of the experimental curve, it has become clear that the experimental result must be influenced by the beam broadening. This prompted the consideration of how the beam size affects the $\bar{\varepsilon}_{xx}$ strain profile, thus generating a composite theoretical map as a function of beam size (see Fig. 3). It is observed that with increasing beam size, the slope of the shoulders decreases symmetrically, accompanied by a decrease in the width of the FT. It is noted that these profiles approach the experimental profile with increasing beam size; a superposition of one theoretical profile with a beam size of 8 nm over the experimental profile appears to fit well (see Fig. 4). Considering a few experimental uncertainties, the experimental strain profile appears to be in reasonable agreement with the theory, indicating that the present theoretical formulation can be applied to explain the experimental result if one considers a variation in the beam size, which is a function of the spot size, beam convergence angle, and specimen thickness.

References

[1] N.V.V. Mogili, D.A. Tanner, and S. Nakahara, Strain 52(2), 162, (2016)

[2] S. P. Timoshenko and J. N. Goodier, Theory of Elasticity, McGraw-Hill Book Co., New York (1970) 53-60, 439-441.

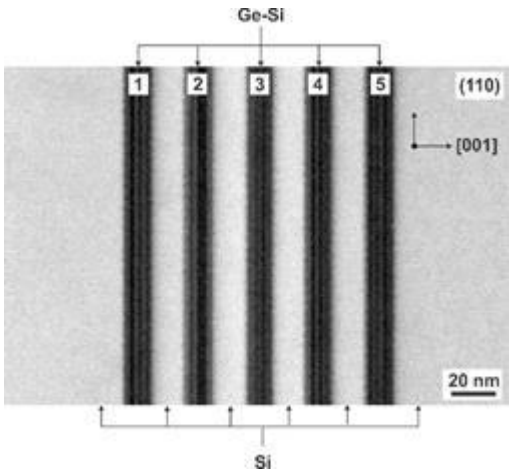

Fig. 1. The bright-field STEM image of the (110) Si cross section containing five layers of Ge-Si/Si SSL.

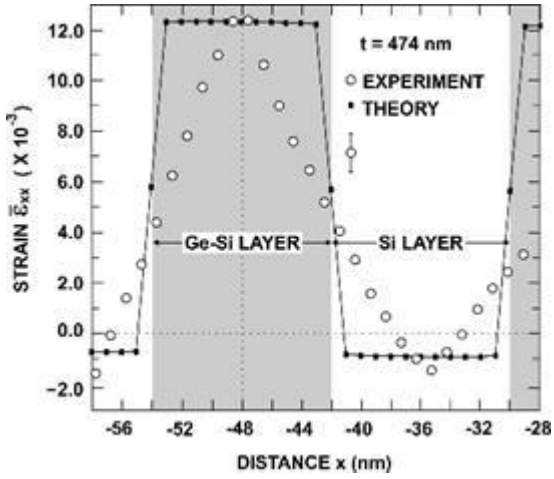

Fig. 2. Experimental and theoretical plots of $\bar{\varepsilon}_{xx}$ around the #1 Ge-Si layer (see Fig. 1). The theory assumes no beam broadening.

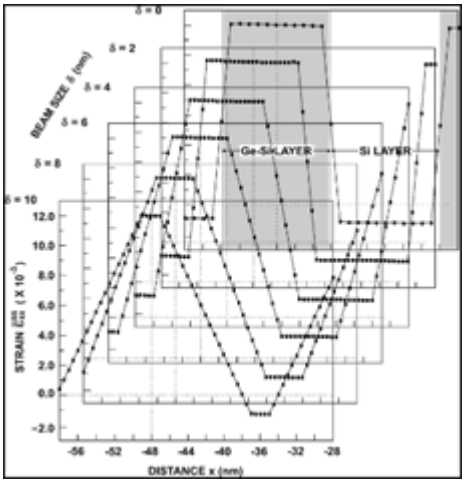

Fig. 3. A theoretical composite map of $\bar{\varepsilon}_{xx}$ plotted as a function of the beam size.

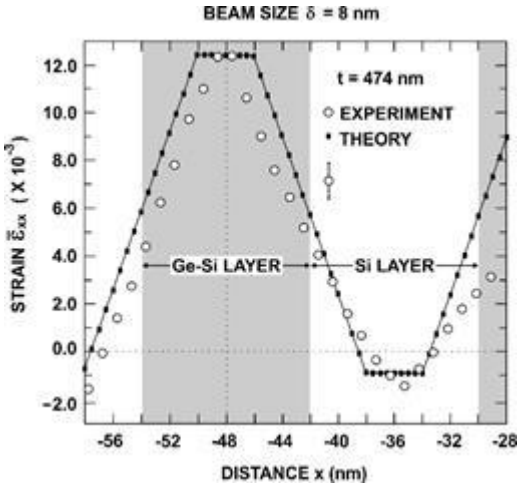

Fig. 4. Comparison of experimental $\bar{\varepsilon}_{xx}$ with the corresponding theoretical plot that assumes the beam size to be 8 nm.